Journal of proteome research

Article

pubs.acs.org/jpr

Evaluation of Data-Dependent and -Independent Mass Spectrometric Workflows for Sensitive Quantification of Proteins and Phosphorylation Sites

Manuel Bauer,[†] Erik Ahrné,[†] Anna P. Baron,[†] Timo Glatter, Luca L. Fava,[‡] Anna Santamaria,[§] Erich A. Nigg, and Alexander Schmidt*

Biozentrum, University of Basel, Klingelbergstrasse 50/70, CH-4056 Basel, Switzerland

Supporting Information

ABSTRACT: In recent years, directed and, particularly, targeted mass spectrometric workflows have gained momentum as alternative techniques to conventional data-dependent acquisition (DDA) LC−MS/MS approaches. By focusing on specific peptide species, these methods allow hypothesis-driven analysis of selected proteins of interest, and they have been shown to be suited to monitor low-abundance proteins within complex mixtures. Despite their growing popularity, no study has systematically evaluated these various MS strategies in terms of quantification, detection, and identification limits when they are applied to complex samples. Here, we systematically compared the performance of conventional DDA, directed, and various targeted MS approaches on two different instruments, namely, a hybrid linear ion trap−Orbitrap and a triple quadrupole instrument. We assessed the limits of identification, quantification, and detection for each method by analyzing a dilution series of 20 unmodified and 10 phosphorylated synthetic heavy-labeled reference peptides, respectively, covering 6 orders of magnitude in peptide concentration with and without a complex human cell digest background. We found that all methods performed similarly in the absence of background proteins; however, when analyzing whole-cell lysates, targeted methods were at least 5−10 times more sensitive than that of the directed or DDA method. In particular, higher stage fragmentation (MS3) of the neutral loss peak using a linear ion trap increased the dynamic quantification range of some phosphopeptides up to 100-fold. We illustrate the power of this targeted MS3 approach for phosphopeptide monitoring by successfully quantifying nine phosphorylation sites of the kinetochore and spindle assembly checkpoint component Mad1 over different cell cycle states from nonenriched pull-down samples.

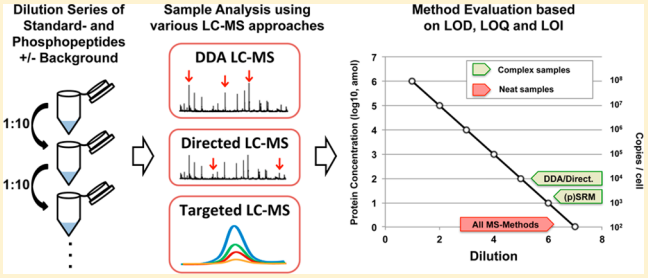

KEYWORDS: *Targeted mass spectrometry, directed mass spectrometry, data-dependent acquisition, peptide quantification, limit of detection, phosphorylation, MAD1, cell cycle*

INTRODUCTION

The identification and precise quantification of low-abundance proteins within whole proteomes is still one of the major challenges of mass spectrometry-based proteomics.[1−6] This can be mainly ascribed to the limited sequencing speed, sensitivity, and dynamic range of current MS instruments in combination with data-dependent acquisition (DDA) LC−MS workflows.[7,8] The recent implementation of directed[9−11] and targeted[9,12,13] LC−MS workflows has tackled some of these limitations and improved the dynamic concentration range over which proteins can be detected and quantified for a selected set of proteins of interest.[10,11,14−16]

In general, the dynamic detection range of DDA-driven workflows critically depends on the sequencing speed of the LC−MS platform employed. This is a result of the stochastic peak selection starting with the most intense precursor ions and the insufficient sequencing capabilities of current LC−MS platforms to acquire MS/MS spectra of all detectable precursor ions in the MS1 survey scans; this, in turn, hampers the identification of low-abundance peptide ion signals when analyzing complex peptide mixtures.[8,17,18] These problems can be largely overcome by data-independent acquisition (DIA) workflows like directed or inclusion list driven LC−MS that allow focused MS sequencing of a specific, predefined set of precursor ion masses independent of their signal intensities. The increased capability to identify low-abundance peptides and proteins of directed over DDA LC−MS has been recently demonstrated on a large scale.[15,19] A significant advantage of directed over targeted MS approaches is the high number of peptides (up to several thousand precursor ion masses) that can be analyzed per run using current high-performance LC−MS platforms.[20,21] On the other hand, the precursor ions have to be detected in the MS1 survey scans to trigger a MS sequencing attempt. This is challenging for low-abundance peptide species

Received: August 18, 2014
Published: October 21, 2014

   dx.doi.org/10.1021/pr500860c | J. Proteome Res. 2014, 13, 5973−5988

within complex mixtures due to the limited intraspectral dynamic detection range.[22,23]

Targeted LC−MS, another DIA strategy, goes one step further and overcomes this limitation by directly monitoring MS/MS product ions without the need to detect peptide precursor ions. The most popular approach is selected reaction monitoring (SRM), in which the precursor ion and fragment ion mass-to-charge (m/z) ratios as well as optimized collision energies are predefined to monitor peptides of interest.[24,25] Once these SRM assays are set up, they can be exchanged between laboratories and instruments[26,27] and thus represent a rich resource for the community.[8,28] Recently, several large-scale studies have been conducted that generated SRM assays for virtually all open reading frames for a number of species and demonstrated the ability of this technique to potentially monitor any protein of a given organism.[8,29,30] Nonetheless, accurate quantification of many low-abundance proteins within very complex protein mixtures still requires additional sample- and time-consuming fractionation/enrichment steps using current LC−MS platforms.[2,20,22,31,32]

Pseudo-selected reaction monitoring (pSRM, also termed product ion monitoring or parallel reaction monitoring (PRM) with high-resolution/accurate mass LC−MS instruments) is another targeted MS approach, in which whole MS/MS spectra are acquired for sets of peptide ion masses of interest.[1,6,33] These spectra can be employed for identification and, by focusing on peptide specific product ions, also quantification. With the ever increasing sequencing speed and resolution of modern Orbitrap and time-of-flight mass analyzers, high-resolution/accurate mass (HR/AM) pSRM/PRM approaches are becoming increasingly popular; because assay development efforts are reduced, fragments suitable for quantification can be selected postacquisition, and the high resolution further increases specificity and quantification confidence.[1,6,13] Recent instruments even allow co-selection, simultaneous fragmentation, and analysis of multiple peptides per MS scan, considerably increasing peptide throughput per LC−MS analysis.[1] Considering the high popularity of the various DIA approaches, it is surprising that no systematic performance assessment, demonstrating the strengths and drawbacks of the individual approaches, has so far been reported.

Here, we present a systematic evaluation of detection, identification, and quantification limits for DDA and several popular DIA MS approaches by analyzing spiked dilution curves covering several orders of magnitude in concentrations of unmodified and phosphorylated peptides. To our knowledge, this is the first study that compares the most popular DDA and DIA approaches systematically and on a quantitative basis. Thus far, this has been done only in a semiquantitative fashion.[7] Our assessment revealed that the high selectivity of HR/AM pSRM considerably improved analytical sensitivity for complex samples and that very sensitive phosphopeptide assays could be established using higher stage fragmentation in linear ion trap instruments. We illustrate the performance of these approaches by monitoring multiple phosphorylation sites of the mitotic spindle assembly checkpoint (SAC) protein Mad1 during different cell cycle stages.

EXPERIMENTAL PROCEDURES

Cell Culture and Sample Preparation of Human Cell Digest

HeLa S3 cells were cultured in Dulbecco's modified Eagle's medium (DMEM, Invitrogen, Carlsbad, CA) supplemented with 10% heat-inactivated fetal calf serum (FCS) and penicillin-streptomycin (100 IU/mL and 100 μg/mL, respectively, GIBCO) at 37 °C in a 5% CO_2 atm in a humidified incubator. Cells (10^7) were collected by centrifugation, and cell pellets were washed twice with PBS. Cells were lysed in 200 μL of lysis buffer (8 M urea, 0.1% RapiGest, 0.1 M ammoniumbicarbonate) using strong ultrasonication, and total protein concentration was determined by BCA assay (Thermo Scientific) according to the manufacturer's instructions. Then, proteins were reduced with 5 mM TCEP for 60 min at 37 °C and alkylated with 10 mM iodoacetamide for 30 min in the dark at 25 °C. After quenching the reactions with 12 mM *N*-acetyl-cysteine, protein samples were digested by incubation with sequencing-grade Lys-C (1:200, w/w; Wako) for 4 h at 37 °C. Samples were diluted 1:4 with 0.1 M ammoniumbicarbonate buffer to reduce urea concentration to 1.6 M, and digestion was continued by adding modified trypsin (1:50, w/w; Promega, Madison, WI) overnight at 37 °C. Subsequently, peptides were desalted on C18 reversed-phase columns according to the manufacturer's instructions (SEP-PAK Vac 3 cc 500 mg, Waters), dried under vacuum, and stored at −80 °C until further use.

Generation of Serial Dilution Mixtures

We took advantage of an ongoing parallel study aimed at the absolute quantification of centrosomal proteins and employed the chemically synthesized 20 heavy-labeled reference peptides (AQUA grade, Thermo Scientific, Table S1) as spike-in standards for our systematic quantitative evaluation of different MS approaches. In this study, for each of the 10 centrosomal proteins of interest, the two full tryptic peptides with the highest MS intensities lacking any missed cleavages were selected as reference peptides. Subsequently, a mixture comprising equal concentrations of all peptides was prepared, and a dilution series was generated using 10-fold steps starting from 0.5 pmol/μL to 0.5 amol/μL. To minimize peptide losses during pipetting and storage, low binding tips (Axygen) and glass vials (VWR International) were applied for all sample preparation steps. Next, the same dilution series was prepared adding the human cell digest sample at a concentration of 0.5 μg/μL to all samples.

In a second dilution experiment, we employed a standard mixture containing 10 singly and doubly phosphorylated peptides in equal amounts (MS PhosphoMix 1 Heavy, Sigma-Aldrich, Table S1) and prepared the same two dilution series (with and without a human cell digest) as described above, starting from 50 fmol/μL to 0.5 amol/μL. Two microliters of each sample was subjected to LC−MS analysis.

Data-Dependent Acquisition (DDA) LC−MS/MS

Peptides were separated on a RP-LC column (75 μm × 20 cm) packed in-house with C18 resin (Magic C18 AQ 3 μm; Michrom BioResources, Auburn, CA, USA) using a linear gradient from 95% solvent A (98% water, 2% acetonitrile, 0.15% formic acid) and 5% solvent B (98% acetonitrile, 2% water, 0.15% formic acid) to 30% solvent B over 40 min at a flow rate of 0.2 μL/min. Each survey scan acquired in the Orbitrap at 60 000 fwhm was followed by 20 MS/MS scans of the most intense precursor ions in the linear ion trap with enabled dynamic exclusion for 20 s. Charge state screening was employed to select for ions with at least two charges and rejecting ions with undetermined charge state. The normalized collision energy was set to 32%, and one microscan was acquired for each spectrum. Collision induced dissociation was

triggered when the precursor exceeded 100 ion counts. The ion accumulation time was set to 300 ms (MS) and 50 ms (MS/MS). All samples were measured in triplicate. Phosphopeptide analysis was carried out as described above with the following modification: each survey scan was followed by 10 MS/MS scans of the most intense precursor ions in the linear ion trap with enabled multistage activation.

Directed (INL) LC–MS/MS

For directed LC–MS/MS, two inclusion mass lists comprising the calculated ion masses of the observed precursor ions of either 20 unmodified (Table S2) or 10 phosphorylated (Table S3) peptides were generated and imported as mass lists to the instrument software. LC–MS analysis was carried out using the same settings as those for DDA analysis with a few modifications: monoisotopic precursor selection was disabled, and peaks with unassigned charge states were not rejected. This helped to trigger more MS sequencing attempts. Furthermore, the ion accumulation time for MS2 scans was set to 100 ms.

Pseudo-selected Reaction Monitoring (pSRM) LC–MS/MS

PRM was carried out in the linear ion trap (LIT) (CID) and Orbitrap (HCD). For both experiments, the peptides and their modifications were imported into Skyline software (version 2.4) (https://skyline.gs.washington.edu/labkey/wiki/home/software/Skyline/page.view?name=default).[17] The precursor ion masses were automatically calculated, and the masses of all observed precursor ions were exported as an instrument method file (Tables S2 and S3). For pSRM-CID-MS2, ion accumulation time was set to 10 ms, and the mass selection window was set to 1 Da. The collision energy was set to 35%, and the activation time was 10 ms. Fragment ions were scanned from the lowest possible m/z to 2000 Th. For pSRM-HCD, MS2 spectra were acquired at a resolution of 7500 (fwhm at 400 m/z), the ion accumulation time was 50 ms, the mass selection window was set to 2 Da, the collision energy was 35%, the activation time was 100 ms, and the measured mass range was from 100 Th to 2 times the precursor mass. Additionally, corresponding charge states were set in the instrument HCD fragmentation method. For pSRM-CID-MS3 analysis, the neutral loss masses were manually calculated and added to the pSRM-CID-MS2 instrument method. Here, to increase sensitivity, the mass selection window was set to 2 Da for MS2/MS3 ion isolation, and an ion accumulation time of 50 ms was applied.

SRM LC–MS/MS (Triple Quadrupole Instrument)

Data derived from a spectral library generated on the basis of acquired HCD spectra of the standard peptide mix from the PRM-HCD experiment were imported into the Skyline program (version 2.4) to extract the corresponding fragment ion masses and precursor ion masses (transitions). After collision energy optimization, the five most suited transitions per peptide were selected according to ref 9 and traced on a triple quadrupole mass spectrometer (QqQ, TSQ Vantage, Thermo Scientific) connected to an electrospray nano ion source and easy nano-LC system (both Thermo Scientific) using the same settings as those used for DDA LC–MS analysis. The cycle time was set to 2 s, resulting in a dwell time of 20 ms per transition. The transition lists with optimized collision energies comprising the 20 unmodified and 10 phosphopeptides are provided as Supporting Information Tables S4 and S5, respectively.

Peptide Quantification

All raw files were loaded into the Skyline software tool (version 2.4) to generate extracted ion chromatograms of the precursor (up to 5) or fragment (up to 10) ions. The mass windows were adjusted to the resolution applied in the corresponding MS method. For PRM-CID methods, a mass window of 0.4 Da was applied. To make the PRM-CID-MS3 data files readable for the Skyline software, we converted the raw files to mzXML format using MM-conversion tool (version 3.9, www.massmatrix.org) and replaced the neutral loss masses used for MS3 by the corresponding original precursor ion masses using an in-house Perl script (available upon request). All integrated peak/transitions were manually inspected and corrected or removed, if required. The integrated and quantified peak/transitions obtained for the different methods and samples are listed in Tables S6–14. Finally, we generated dilution profile correlations and applied an established algorithm[19] to determine LOQ and LOD values as well as linear correlations (Pearson's correlation coefficient (R^2) from highest concentration to LOQ) for each MS method and peptide analyzed (Figures S3–S11).

Determination of Identification Limits

All raw files acquired by DDA, INL, and pSRM for the dilution curve samples of unmodified peptides were converted to mgf format using the MM-conversion tool (version 3.9, www.massmatrix.org) and searched against a decoy (consisting of forward and reverse protein sequences) human Swiss-Prot database (download date 16/05/2012) containing known contaminants, resulting in a total of 41 250 protein sequences using Mascot (Matrix Science, version 2.4). The search parameters were set as follows: full tryptic specificity was required (cleavage after lysine or arginine residues unless followed by proline); up to two missed cleavages were allowed; carbamidomethyl (C) was set as fixed modification; oxidation (M), label $^{13}C(6)^{15}N(2)$ (K), and label $^{13}C(6)^{15}N(4)$ (R) were set as variable modifications; 10 ppm precursor mass tolerance; and 0.6 (0.02) Da fragment mass tolerance for CID (HCD) tandem mass spectra. After importing the data to Scaffold software (http://www.proteomesoftware.com, version 4.2.1), the FDR rate was set to <1% for MS/MS spectra identifications by the Scaffold Local FDR algorithm based on the number of decoy hits. All identified MS/MS spectra in the dilution curve experiment for DDA, INL, and pSRM are available as Tables S15–S17.

Monitoring of Mad1 Phosphorylation Sites

Cell Culture, Synchronization, and Kinase Inhibitors. HeLa S3 cells were cultured as described above. Cell cycle arrest in S-phase was induced by thymidine (2 mM, Sigma-Aldrich) treatment for 24 h. For MS analysis of mitotic cell cycle stages, cells were released from thymidine and arrested in mitosis before harvesting. Mitotic arrest in prometaphase was induced by nocodazole (0.5 μg/mL, Sigma-Aldrich) treatment for 14 h after thymidine release. Mitotic cells were collected by mitotic shake-off. Mitotic arrest in metaphase was induced by addition of the proteasome inhibitor MG132 (10 μM, Calbiochem) for 2 h, which was added 10 h after thymidine release.

Cell Extracts and Immunoprecipitations. For preparing extracts, HeLa S3 cells were washed once with ice-cold PBS and resuspended in ice-cold lysis buffer (20 mM Tris, pH 7.4, 150 mM NaCl, 0.5% IGEPAL CA-630, 1 mM DTT, 30 μg/mL RNase, 30 μg/mL DNase, protease inhibitor cocktail (Roche, 1

dx.doi.org/10.1021/pr500860c | J. Proteome Res. 2014, 13, 5973–5988

EDTA-free tablet for 10 mL of lysis buffer) and phosphatase inhibitors cocktail (cocktails 2 and 3; Sigma-Aldrich)) and incubated for 30 min on ice. After cell lysis, suspensions were cleared by centrifugation at 14 000 rpm for 15 min. Immunopurification of endogenous Mad1 was performed using 50 μL of solid Affi-Prep protein G matrix beads (Bio-Rad Laboratories) chemically cross-linked to 1 μg/μL of antibody[12] against 1 to 2 mg of clarified cell lysate for 2 h at 4 °C. Afterward, the resin was washed with lysis buffer followed by washing with HNN buffer (50 mM Hepes, pH 7.5, 150 mM NaCl, 5 mM EDTA, 50 mM NaF). Proteins were eluted with 100 mM glycine, pH 2.8, neutralized by the addition of Tris buffer (pH 8.0), reduced, alkylated, enzymatically cleaved, and prepared for MS analysis as described above. For generating a comprehensive phosphorylation site map of Mad1, immune-purified proteins obtained from 10 (S-phase) and 15 (prometaphase and metaphase) 15 cm dishes were pooled, divided in two aliquots, and subjected to the two different phosphopeptide enrichment strategies described below. For monitoring of Mad1 phosphorylation sites, sufficient protein amounts could be obtained from one (S-phase) and two (prometaphase and metaphase) 15 cm dishes. After sample preparation, the peptide samples were dissolved in 40 μL of 0.1% formic acid containing 125 fmol/μL of each heavy-labeled phosphopeptide.

Western Blot. HeLa S3 cells were synchronized with thymidine and subsequently released into nocodazole for 14 h. Cells were collected by mitotic shake-off, and Mad1 and associated proteins were immunopurified from mitotic extracts. The following antibodies were used for western blot: mouse anti-Mad1,[12] rabbit anti-Mad2 (Bethyl Laboratories, cat. no. A300-301A, 1 μg/mL), and mouse anti-α-tubulin (Sigma-Aldrich, cat. no. T9026, 0.2 μg/mL).

Phosphopeptide Enrichment (TiO_2). Thirty microliters of titanium dioxide beads (100 mg/mL, Titansphere, GL Sciences Inc., Japan) was placed on self-made GELoader tips (Eppendorf) plugged with a piece of C8 material (Empore, 3M, 3 M Empore C8 and C18 disks, 2214-C8, Bioanalytical Technologies, St. Paul, MN). The columns were washed with water (HPLC grade, Sigma-Aldrich), methanol, and a solution of 80% ACN (Acetonitrile) and 2.5% TFA (trifluoroacetic acid) saturated with phthalic acid. Digested and dried peptides were reconstituted in 80% ACN and 2.5% TFA saturated with phtalic acid and loaded on the microcolumns. To allow maximal binding of phosphorylated peptides to the titanium dioxide beads, the peptide−bead mixture was incubated for 10 min and then slowly passed through and applied two additional times. The microcolumns were subsequently washed with a mixture of 80% ACN and 2.5% TFA saturated with phthalic acid, a mixture of 80% ACN, 20% water, and 0.1% TFA, and, finally, with 0.1% TFA. Phosphorylated peptides bound on the TiO_2 were eluted with a 0.3 M ammonium hydroxide solution. Phosphopeptide-enriched eluates were immediately acidified with 2 M HCl and 5% TFA, desalted, purified on C18 microspin columns (Harvard Apparatus), and dried in a SpeedVac concentrator.

Phosphopeptide Enrichment (IMAC). PHOS-select iron affinity gel beads (Sigma-Aldrich) and dried peptides were resuspended in 30% acetonitrile/250 mM ethanol. IMAC beads and peptides were shaken at room temperature at 1400 rpm for 2 h. Subsequently, samples were loaded three times in a constricted GELoader tip and washed four times with 30% acetonitrile/250 mM ethanol. Phosphorylated peptides were eluted using 50 mM Na_2HPO_4/NH_3 (pH 10.0), acidified with 100% ethanol and 10% TFA (pH < 3.5), desalted, and passed to LC−MS/MS analysis.

Generation of a Mad1 Phosphorylation Site Catalogue from Phosphopeptide-Enriched Samples. One microgram of total phosphopeptides was subjected to DDA LC−MS/MS using HCD and CID with enabled multistage activation fragmentation, as specified above. Acquired raw files were database-searched using Mascot and Scaffold software, as described above, with the following parameter modification: oxidation (M), label $^{13}C(6)^{15}N(2)$ (K), label $^{13}C(6)^{15}N(4)$ (R), and phosphorylation (S, T, Y) were set as variable modifications. The identified proteins, peptides, and MS/MS-spectra (Tables S18−S20) were filtered to a FDR of 1% according to the Scaffold Local FDR algorithm based on the number of decoy hits. A list of all MS/MS spectra assigned to Mad1 phosphopeptides is shown in Table S21, and a summary list comprising all identified Mad1 phosphorylation sites is illustrated in Table 1. Protein probabilities were assigned by the ProteinProphet program.[34] Proteins that contained similar peptides and could not be differentiated on the basis of MS/MS analysis alone were grouped to satisfy the principles of parsimony. Proteins sharing significant peptide evidence were grouped into clusters. The location of the phosphorylated residues was automatically assigned by Mascot (score >10). All annotated spectra, MS raw files, and search parameters employed have been deposited to the ProteomeXchange Consortium (http://proteomecentral.proteomexchange.org) via the PRIDE partner repository[35] with the data set identifier PXD000964 and DOI 10.6019/PXD000964.

Mad1 Phosphorylation Site Monitoring. Heavy-labeled reference peptides were synthesized for all identified phosphopeptides of Mad1. For precise quantitation of the single-serine phosphorylation sites at positions S484, S485, S486, and S490, we ordered all possible monophosphorylated versions of the corresponding heavy reference peptide (SQSSSAEQSFLFSR, Table 1). All different phosphopeptide sequences and modifications together with the identified MS/MS spectra from the previous phosphorylation catalogue experiment were imported into Skyline software (version 2.4) to set up a pSRM method to monitor all phosphopeptides. In an initial analysis, we carried out MS2- and MS3-based PRM analysis to select for the best transitions for each peptide. Because of their higher selectivity and lower noise levels, transitions originating from MS3 scans were preferred, if available. Phosphopeptides were quantified using the Skyline tool and the same parameters as described above. The quantitative results, including normalization, ratio determination, and statistical analysis, are summarized in Tables S22 and S23.

For the determination of phosphorylation site stoichiometries and to compensate variations in Mad1 concentrations, additional label-free quantification experiments of the same samples were carried out as described recently.[36] In brief, 1 μg of peptides was subjected to DDA LC−MS/MS analysis using CID with enabled multistage activation fragmentation and the same LC and MS settings as specified above. LC−MS Progenesis software (version 4.1.4832.42146) in combination with the Mascot database search tool (version 2.4) was employed to identify and quantify unmodified and modified Mad1 peptides using the same database search parameters for phosphopeptides as described above. Importantly, the Progenesis software was set such that only nonconflicting peptides

with specific sequences for single proteins in the database were employed for quantification. The results were further statically validated by our in-house software tool SafeQuant (available upon request), as recently shown.[36] All identified and quantified peptides are listed in Table S24. Differences in Mad1 concentrations in the samples were normalized using the sum of all MS intensities generated from Mad1 peptides. The corresponding normalization factors using the first sample as base are displayed in Table S23. The data file names of LC−MS runs of all samples analyzed in this study are shown in Table S25.

RESULTS AND DISCUSSION

Experimental Overview

The general aim of this study was to assess the capabilities of three recently established LC−MS strategies in terms of sensitivity and linear relative quantification range for a variety of different peptides in the presence and absence of a complex analytical background (Figure 1). Therefore, we prepared serial dilutions of two different peptide mixtures consisting of 20 unmodified and 10 phosphorylated chemically synthesized heavy peptides (for selection criteria, see Experimental Procedures) covering a concentration range of 6 and 5 orders of magnitude, respectively (referred to as neat samples). To assess analytical performance under a more realistic scenario, we prepared the same dilution series with a complex human digest spiked into each sample (referred to as complex samples). This allowed us to precisely determine the impact of the analytical background on limit of detection (LOD), quantification (LOQ), and identification (LOI) for each peptide and MS approach applied in this study. The four dilution series were analyzed in duplicate using the following data-dependent (DDA) and -independent acquisition (DIA) MS approaches. (i) In DDA, only peptides of the highest intensities in the acquired survey scans are selected for MS sequencing, whereas many other peptides of sufficient intensity for identification pass through the instrument to remain unidentified. (ii) A directed LC−MS/MS strategy (also termed inclusion mass list driven, INL) that attempts to overcome this limitation by directing MS sequencing to the precursors of interest independent of their MS intensities using an inclusion mass list.[10,11,14,15] Although several thousand peptides can be analyzed by this approach, a drawback is the necessity to detect the precursor ions in the MS1 survey scans to trigger fragmentation. (iii) Targeted LC−MS/MS methods (selected reaction monitoring (SRM) and pseudo-selected reaction monitoring (pSRM, like SRM, but a full MS/MS scan is acquired) that directly fragment selected peptide ions and use the corresponding fragment ions for identification and quantification. We analyzed each sample by SRM using a triple quadrupole (QqQ) MS and by pSRM using collision induced dissociation (CID, ion detection in the linear ion trap (LIT)) based fragmentation. For phosphopeptide analysis, we additionally carried out higher energy collision dissociation (HCD, ion detection in the orbitrap) and neutral loss MS2/MS3 CID fragmentation in the LIT. All peptides were quantified using Skyline,[17] and fragment spectra were identified by database searching. Finally, we generated dilution profile correlations for each peptide and MS method and applied an established algorithm[19] to determine linear quantification ranges as well as identification, quantification, and detection limits.

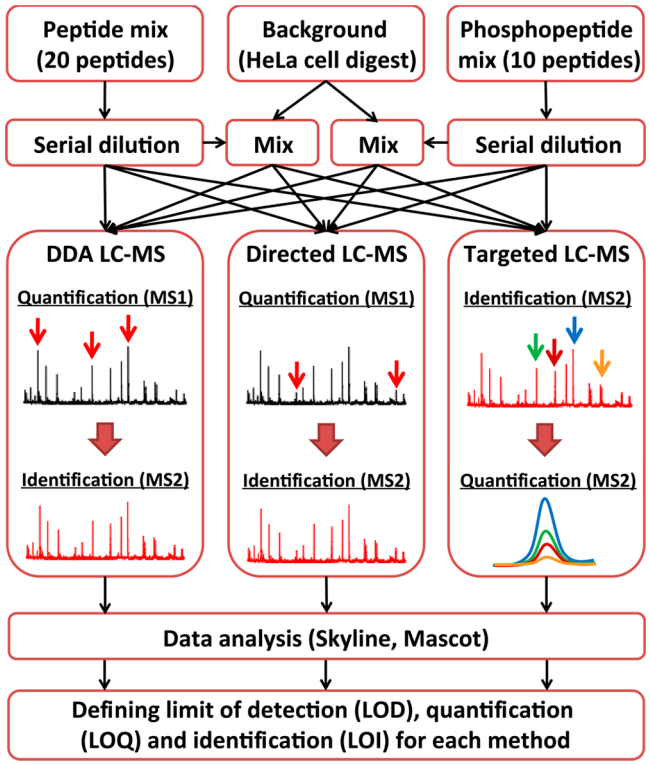

Figure 1. Experimental overview. Two dilution series were generated from two mixtures containing equal amounts of (i) 20 unmodified and (ii) 10 monophosphorylated, respectively, heavy-labeled reference peptides. Additionally, a HeLa whole-cell extract was prepared, digested with trypsin, and spiked into each dilution series sample. The mixtures were analyzed by liquid chromatography−tandem mass spectrometry using three distinct methods to quantify the peptides of interest: data-dependent acquisition (DDA), directed or inclusion list driven (INL) LC−MS, and various targeted LC−MS workflows. These include selected reaction monitoring (SRM) on a triple quadrupole instrument, pSRM on a linear ion trap (LIT) and Orbitrap instrument, and higher stage fragmentation for phosphopeptides on a LIT instrument. For all methods, peak integration and quantification were carried out using the Skyline software suite,[17,29,30] and full MS/MS spectra were database-searched by the Mascot search engine for identification.[2,20,22,54] From this data, limits of detection, quantification, and identification were determined for each LC−MS method and dilution series using recently established algorithms.[1,6,19,33]

Impact of Analytical Background on Limit of Detection/Quantification of Unmodified Peptides

First, we assessed the effect of the analytical background on the dynamic detection and quantification range of the four popular MS approaches. This included data-dependent acquisition (DDA); directed, inclusion mass list driven peak selection (INL); selected reaction monitoring (SRM) on a QqQ; and pSRM (pSRM-CID) on a LIT LC−MS platform. We determined LODs and LOQs for all peptides and every MS strategy in the presence and absence of a complex human cell digest. In general, we found a very high and linear correlation of peak intensity and analyzed peptide amounts for all MS approaches employed down to the low attomole level (Figures S3−S6). A typical example is illustrated in Figure 2A. For this peptide, LOD/LOQ were found to be in the low attomole range when analyzed by SRM (Figure 2A). However, LOD/LOQ increased by a factor of 10 when analyzing this peptide in the context of a complex human digest (Figure 2B). The observed trend of elevated LOD/LOQ values with increased

dx.doi.org/10.1021/pr500860c | J. Proteome Res. 2014, 13, 5973−5988

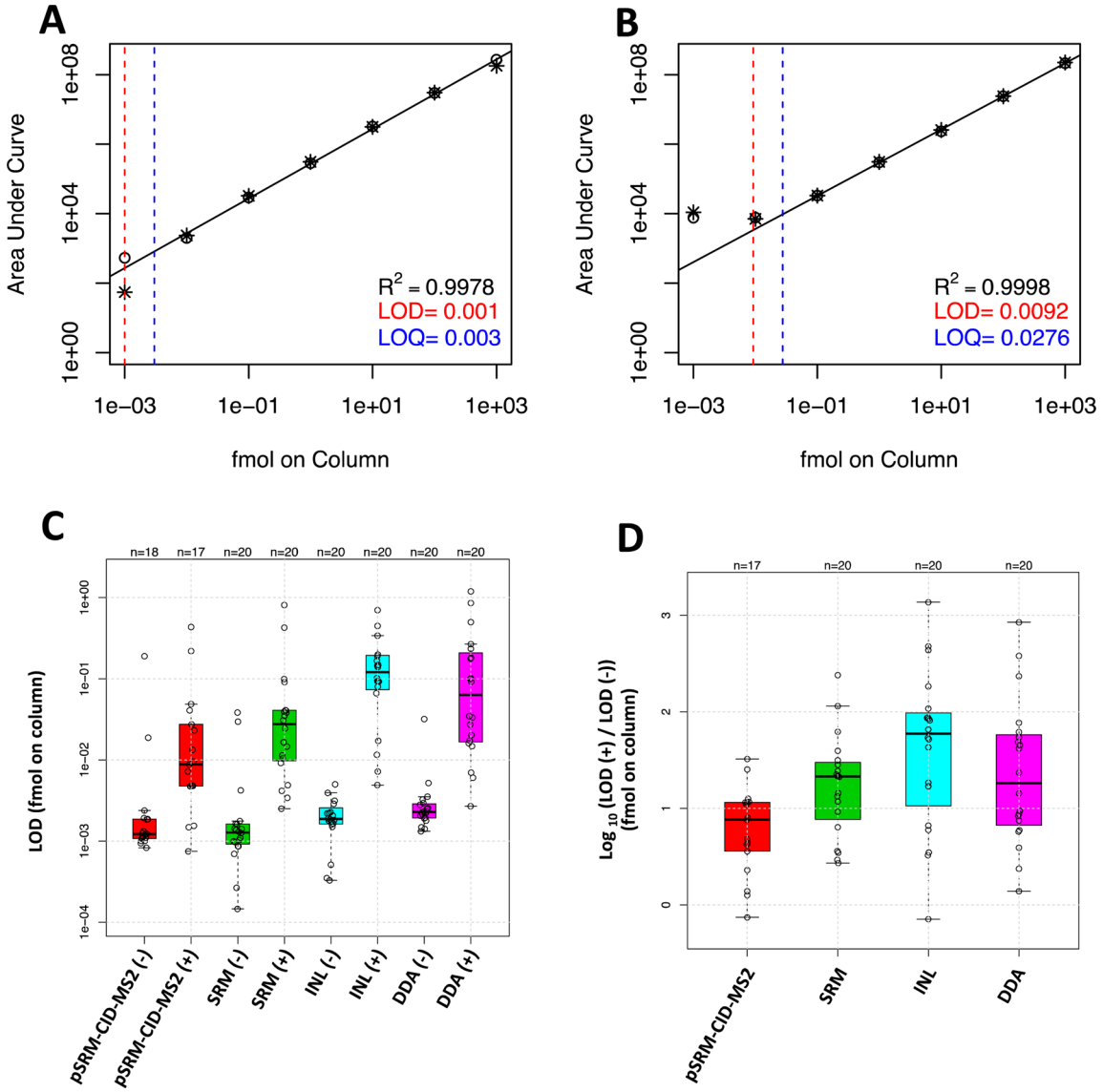

Figure 2. Defining detection and quantification limits for unmodified peptides. The peak intensities and peptide concentrations were plotted for each peptide and LC−MS method to compute linear regression (squared Pearson correlation (R^2) from highest concentration to LOQ) as well as limit of detection (LOD) and limit of quantification (LOQ). (A) Plot of the peptide INEVLAAAK analyzed by SRM in the neat dilution series. The R^2, LOD (red), and LOQ (blue) are indicated. (B) Similar to panel A for the same peptide analyzed in the context of complex human cell digest. (C) Box plot showing the LOD values obtained for the four different LC−MS methods applied for the neat (−) and complex (+) dilution series. The box covers the lower and higher quartiles. The median LODs are indicated as a black bar. The whiskers correspond to the maximum and the minimum values, excluding outliers. Outliers that exceed 1.5 times the lower or upper quartile were not considered and are shown as black circles. (D) Similar to panel C, showing the impact of the complex analytical background on the individual LOD values of each MS method.

sample complexity was confirmed for all peptides (Figure 2C). Although all four methods achieved similarly low LODs/LOQs with neat samples, LODs/LOQs increased in the complex samples to the mid attomole range for the targeted MS approaches and high attomole range for MS1-based quantification approaches (DDA and INL, Figure 2C). The lesser increase in LOD/LOQ of the targeted MS methods is expected, as these approaches do not need to detect the precursor ions in the MS1 survey scans and have a higher selectively due to the double mass filtering applied. Nonetheless, the performance of targeted approaches is also affected by the analytical background present in the sample and considerably decreases the sensitivity of peptide assays by 10-fold for pSRM-CID and 20-fold for SRM. Therefore, like DDA-based analysis, reduction of complexity (e.g., by sample fractionation,[20] immune purification/depletion,[22] or use of longer LC columns[24]) is an efficient way to increase the sensitivity of targeted MS assays in complex mixtures. An advantage of the pSRM approach over SRM is that less prior information is required to set up the assays (basically, the peptide ion masses are sufficient) and transition selection can be carried out after the LC−MS analysis.[1,6] This allowed us to remove outliers and pick the most intense fragment ions for quantification postanalysis. By contrast, fragment ion masses and their fragmentation parameters have to be defined before SRM-based analysis. In line with previous studies,[26] popular and ubiquitous LIT−MS achieved very good sensitivities, making them a suitable alternative for targeted MS analysis in the event that QqQ instruments are not available. However, the current sequencing speed of LIT does not match the number of transitions monitored by SRM on a QqQ

dx.doi.org/10.1021/pr500860c | J. Proteome Res. 2014, 13, 5973−5988

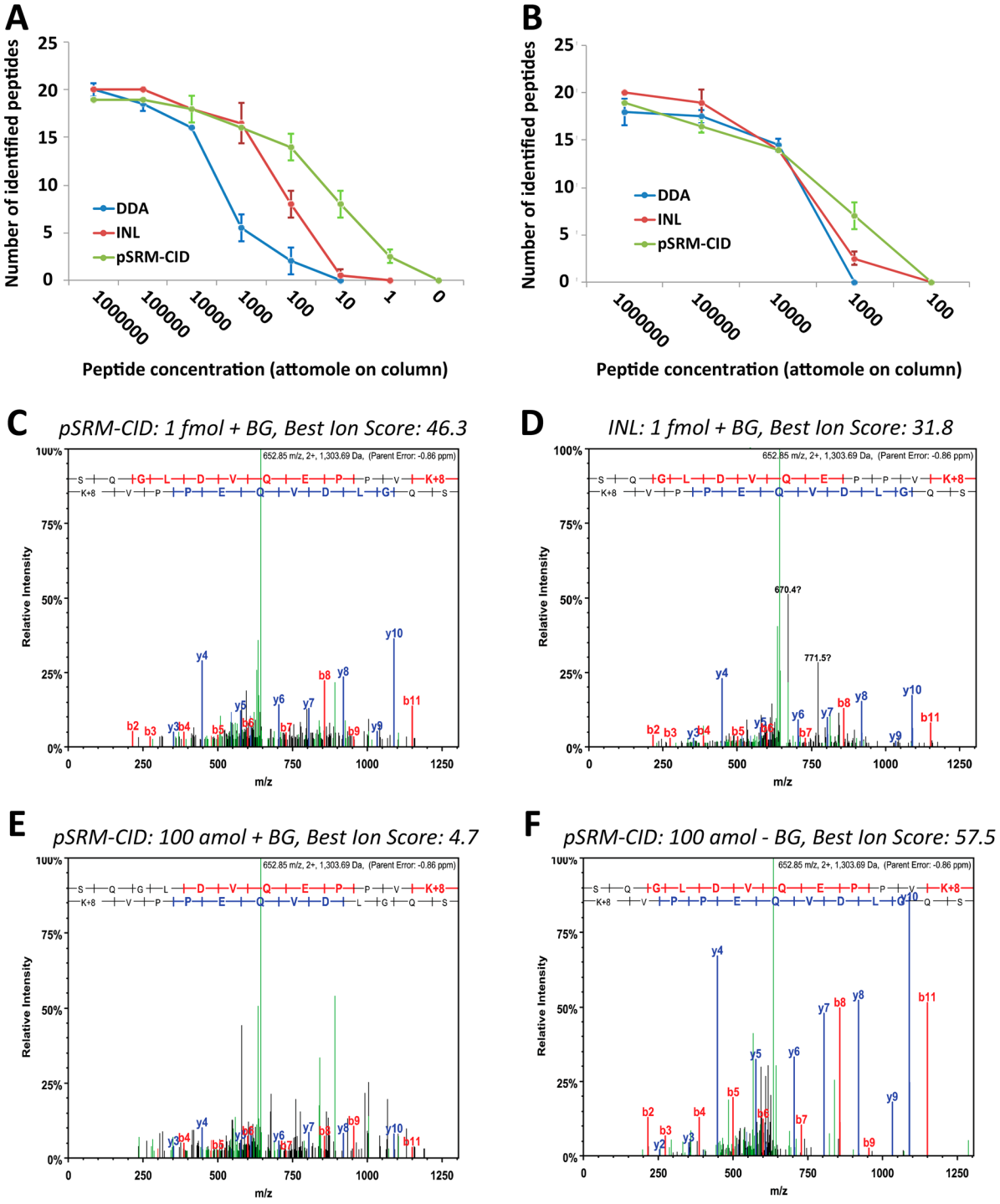

Figure 3. Defining limits of identification for unmodified peptides. (A) The graph shows the number of peptides correctly assigned by the database search tool dependent on their concentration for three different LC−MS approaches and the neat dilution series. (B) Similar to panel A, but for the complex dilution series samples. (C) MS/MS spectrum acquired by pSRM-CID having the highest Mascot ion score (46.3) for the heavy (*Lys-8) peptide SQGLDVQEPPVK* at 1 fmol concentration in the complex sample. (D) Similar to panel C, obtained by directed (INL) LC−MS at 1 fmol concentration in the complex sample. (E) Similar to panel C, but at 100 amol concentration acquired from the neat sample. (F) Similar to panel C, but acquired in the complex sample at a 10-fold lower concentration (100 amol).

instrument and therefore fewer peptides can be monitored by pSRM than by SRM. In our study, around 2.5 (5) times more peptides could be quantified by SRM (5 transitions per peptide) compared to that by pSRM-CID (HCD) in a single LC−MS run.

Naturally, since DDA and INL differed only in the way the precursor ions were picked for MS/MS analysis, both approaches showed similar LOD/LOQ values determined from the MS1 spectra (Figure 2C). The smaller LOD/LOQ loss and the slightly lower LOD/LOQ values observed for the DDA method in the complex samples (Figure 2C,D) could be explained by the higher resolution applied for the DDA approach (60 000 at 400 m/z (fwhm)) compared to that for INL (30 000 at 400 m/z (fwhm)). Because, in a normal DDA/

dx.doi.org/10.1021/pr500860c | J. Proteome Res. 2014, 13, 5973−5988

INL LC−MS experiment, each peak has to be identified by MS sequencing to be assigned for analysis, these LOD and LOQ values do not represent the true dynamic range usually achieved by these methods. Therefore, defining limits of identification (LOI) will result in a more meaningful assessment and comparison of these two approaches. This will be further investigated below.

To conclude, all methods achieved similar LODs/LOQs in the low-complexity samples, and these values increased considerably with higher sample complexity. As expected, targeted methods are less affected by analytical background than that of the DDA and INL approaches. Nonetheless, the sensitivity of SRM assays will also benefit considerably from a reduction of sample complexity. On average, for complex samples, LODs/LOQs of targeted approaches were 5−10-fold lower than those of DDA/INL approaches for the peptides analyzed in this study.

Determining Limit of Identification for Unmodified Peptides

As mentioned above, LOI is a better indicator to assess the performance of the INL and DDA methods. To define LOIs, we searched all MS/MS spectra acquired with the DDA, INL, and pSRM-CID approaches against a human database and applied a peptide false discovery rate of 1% to all samples (see Experimental Procedures). When analyzing low-complexity samples, more peptides were identified at low concentrations using the INL approach compared to that using DDA (Figure 3A). In particular, in the mid concentration range at 1000 amol, almost all peptides were identified by INL, whereas DDA identified only 6 out of 20. Further zooming in on this issue, we found that, at low concentrations, many peptides were not fragmented by DDA and therefore were not identified. Apparently, disabling most peptide ion detection filters of the instrument software (see Experimental Procedures) resulted in more identifiable peptide specific MS/MS scans from the inclusion mass list for very low-intensity signals. This suggests that implementing more sophisticated peak detection algorithms for peptide ions could increase the overall sensitivity of DDA LC−MS. The lowest LOIs could be achieved by pSRM-CID, indicating that meaningful MS/MS spectra could be generated in the highly sensitive LIT even if no precursor ion was detectable in the survey scan acquired in the less sensitive Orbitrap. Therefore, to exploit the full sensitivity of an LIT in the hybrid LC−MS platform employed, a more sensitive Orbitrap would be beneficial to further improve LOIs for DDA/INL in low-complexity samples.

Compared to neat samples, LOIs increased significantly for all approaches upon higher sample complexity, and only minor differences in identification limits were observed across the three methods (Figure 3B). This indicates that limited MS/MS scan speed (tackled by the INL approach) and triggering of MS/MS spectra (overcome by the pSRM-CID approach) had only a minor impact on identification rates when analyzing complex samples. Interestingly, LOIs were, on average, 10−100-fold higher than the corresponding LODs, suggesting that many precursor ions that were easily detectable in the MS1 scan and consequently fragmented remain unidentified by database searching (Figure 2C). Therefore, we next investigated if the interpretation of these MS/MS spectra by the database search software was hampered at low peptide concentrations. A typical example is shown in Figure 3C. At a concentration of 1 fmol, the peptide could be unambiguously identified by pSRM and INL in the complex sample with the corresponding fragment ions dominating the MS/MS spectrum (Figure 3C,D). After reducing the concentration by 10-fold, the fragment ions, albeit present, were masked by interfering peaks, which complicated the interpretation of this MS/MS spectrum and resulted in an insignificant Mascot ion score (Figure 3E). Without background, high-quality MS2 scans are obtained at this low concentration (Figure 3F). From this, one can conclude that the ratio of precursor-specific fragments to all fragment ions present in the MS/MS spectra is a far more critical parameter for the successful identification of low-abundance peptide species within complex samples than is MS/MS scan speed or dynamic detection range within the MS1 scan. As a result, the increasing prevalence of interfering peaks ultimately defines LOIs for the DDA and INL approaches evaluated in this study. This is in line with a recent publication showing that MS/MS spectra become progressively more difficult to identify if precursor ion intensity is lower than the sum of all other co-fragmenting ions within the mass selection window. The authors further report that this was the case for the large majority of MS/MS spectra acquired in a single-shot LC−MS/MS analysis.[8] Consequently, reducing the amount of co-fragmenting peptides by applying smaller mass selection windows,[8] using software that can identify multiple co-fragmenting peptides from the same MS2 spectra,[31,32] extracting co-eluting peptides,[8,37] or using fragment ion-specific search tools[10,11,38,39] are useful approaches to extract the relevant fragment ions from noisy spectra and improve the identification rate of low-abundance peptides for these types of analyses. Furthermore, spiking in heavy reference peptides at high concentrations that are amenable to database searching is an effective way to assign the corresponding precursor/fragment ions of the endogenous peptide and considerably improve analytical sensitivity, as demonstrated for the INL approach.[40]

To conclude, besides limited sequencing speed and dynamic detection range, co-fragmentation of peptides with similar ion masses and elution profiles contributed, to a large extent, to the high LOIs observed when analyzing complex samples. Smaller mass selection windows and adequate software tools that extract relevant fragment ions will be useful to lower LOIs; however, for very complex samples, co-fragmentation will remain a major challenge for single-dimension LC−MS analysis.[8,15,16] Notably, because only correctly identified peptides are amenable to quantification in standard DDA and INL workflows, the LOIs actually define the LODs/LOQs achieved in our experimental setup for these two MS methods. With LOIs being in the low femtomole range, the actual LODs/LOQs achieved by the DDA and INL methods were therefore several fold higher than those determined solely from the precursor ions in the MS1 scans.

Impact of Analytical Background on Limit of Detection/Quantification of Phosphopeptides

Although the SRM and the corresponding pSRM methods showed the highest sensitivity for monitoring unmodified peptides within complex mixtures, we next asked if this was also the case for modified peptide species with altered fragmentation patterns. To evaluate this, we employed a commercial mix comprising 10 absolutely quantified phosphopeptides carrying single or multiple phosphorylations, as identified in a recent large-scale study using LIT-based fragmentation.[8,18,41] To

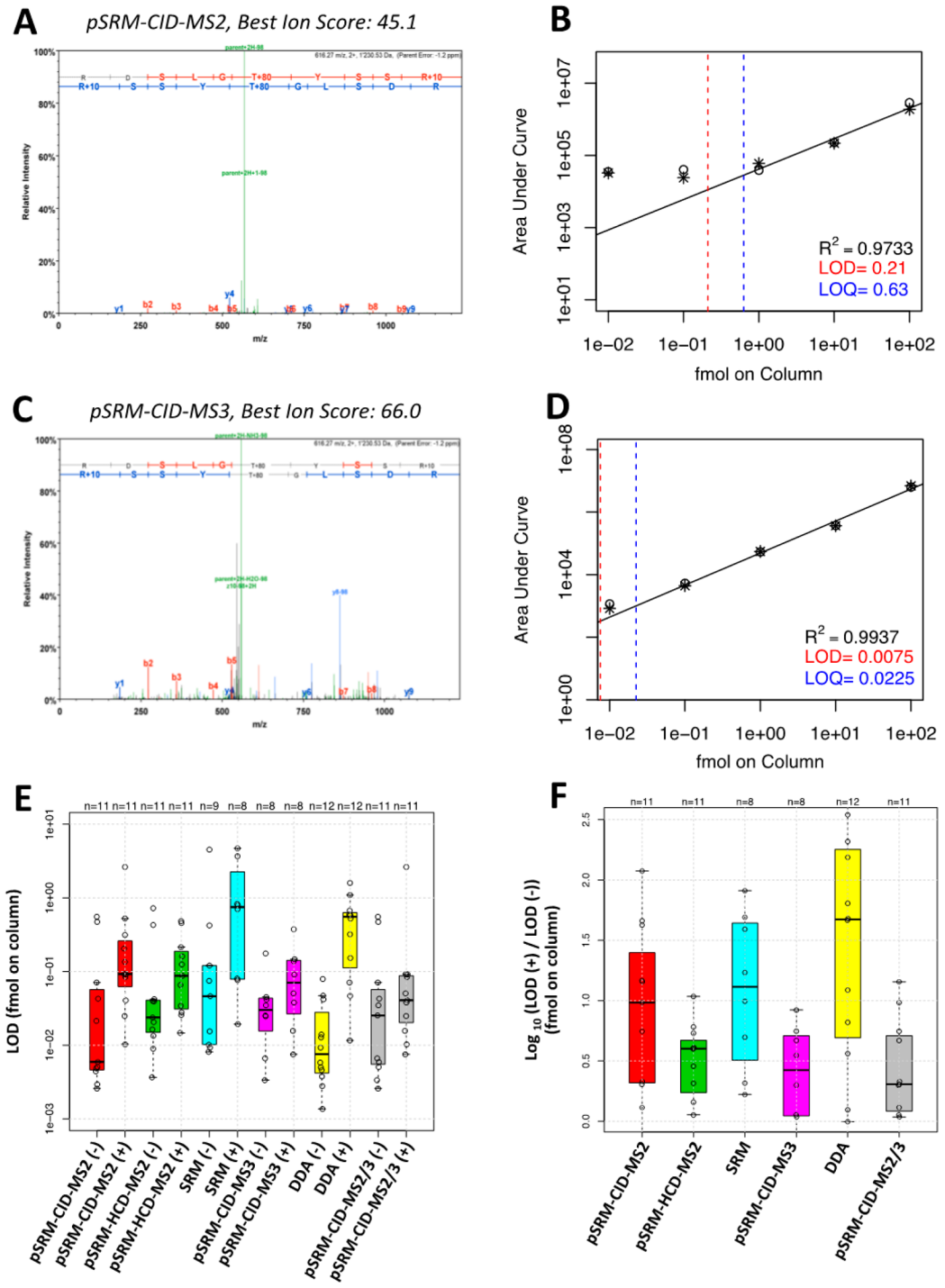

Figure 4. Defining detection and quantification limits for phosphorylated peptides. (A) MS/MS spectrum acquired by pSRM-CID-MS2 of the heavy (*Arg-10) phosphopeptide RDSLGpTYSSR* in the neat sample and assigned with the highest Mascot ion score (45.1). The assigned b- (red) and y-ions (blue) as well as the neutral loss peaks (green) are indicated. (B) Plot of the peak intensities and concentrations of the heavy (*Arg-10) phosphopeptide RDSLGpTYSSR* using the pSRM-CID-MS2 approach. The computed linear regression (squared Pearson correlation (R^2) from highest concentration to LOQ) as well as limits of detection (LOD) and quantification (LOQ) are shown. (C) MS3 spectrum acquired from the neutral loss peak of the same phosphopeptide having the highest ion score (66.0). The assigned b- (red) and y-ions (blue) as well as the neutral loss peaks (green) are indicated. (D) Similar to panel B, but for the pSRM-CID-MS3 method. (E) Box plot showing the LOD values obtained for the 6 different LC−MS methods applied for the neat (−) and complex (+) dilution series. The box covers the lower and higher quartiles. The median LODs are indicated as a black bar. The whiskers correspond to the maximum and the minimum values, excluding outliers. Outliers that exceed 1.5 times the lower or the upper quartile were not considered and are shown as black circles. (F) Similar to panel E, showing the impact of the complex analytical background on the individual LOD values of each MS method.

minimize sample consumption and cost, we prepared a 10-fold dilution series starting from 100 fmol down to 1 amol.

We added two more targeted MS analysis methods to our evaluation that are specifically suited for phosphopeptide analysis, namely, higher stage fragmentation (MS3)[15,42] and

dx.doi.org/10.1021/pr500860c | J. Proteome Res. 2014, 13, 5973−5988

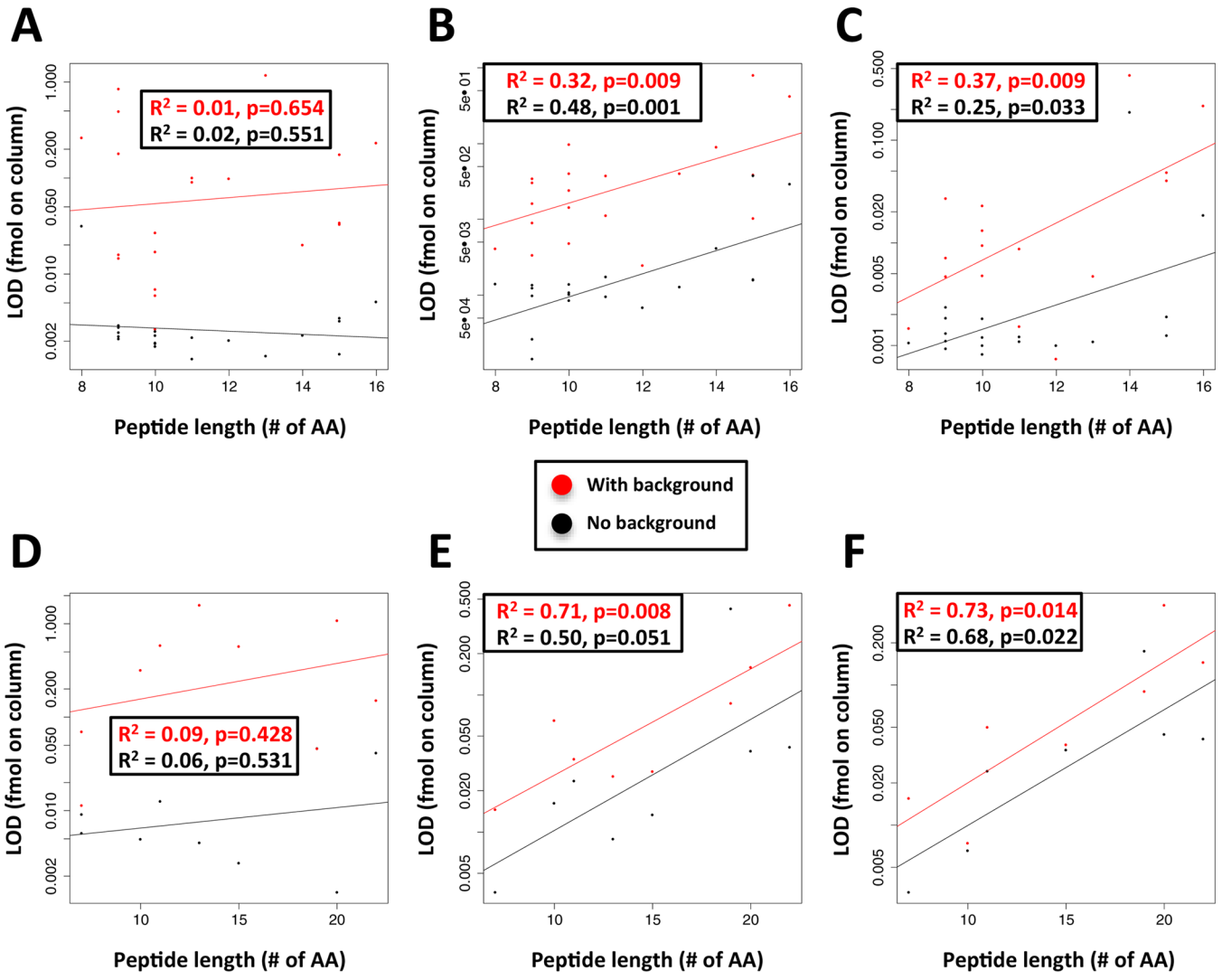

Figure 5. Dependence of peptide length on the limits of detection achieved for the different samples and best performing methods. For each peptide, the number of amino acids against the LODs achieved in the complex (red) and the neat (black) dilution series samples is shown. The plots for 20 unmodified peptides analyzed by DDA (A), SRM (B), and pSRM-CID-MS2 (C) are shown. The same plots are illustrated for the phosphopeptide dilution series analyzed by DDA (D), pSRM-HCD-MS2 (E), and pSRM-CID-MS3 (F). The trend lines and squared Pearson correlations (R^2) as well as the p-values are indicated for each plot and dilution series, respectively. We performed an ordinary least-squares regression, describing log(LOD) as a function of log(peptides length) (formally, log(LOD) = k log(PepLength) + m). The calculated p-value is the probability that the slope parameter k equals 0 given the observed data.

high-resolution higher energy collision dissociation (HCD).[21,43] We performed MS3 of neutral loss peaks that frequently dominate CID spectra of serine and threonine phosphorylated peptides and thereby mask peptide-specific fragment ions required for identification and quantification.[23,42,44] This method has been recently demonstrated to be well-suited for quantification of selected phosphopeptides by targeted MS.[25,45] We observed neutral loss peaks in 8 of the 11 MS/MS spectra identified and generated MS3-based pSRM assays for the corresponding peptide ions. The higher selectivity gained by the additional fragmentation step can be nicely demonstrated in Figure 4. The phosphopeptide RDSLGpTYSSR showed a strong neutral loss peak in the MS2-CID spectra, which masked sequence-specific fragments amenable for quantification (Figure 4A). Conversely, the MS3 spectra of the neutral loss peak generated a concert of fragment ions suited for identification and quantification (Figure 4C). Switching from pSRM-CID-MS2 to MS3-based analysis decreased LOD/LOQ in the complex samples for this peptide by almost 2 orders of magnitude, down to the low attomole range (Figure 4C/D). As is apparent from Figure 4D, this additional mass filter lowered LOQs without compromising the linearity of quantification. The additional fragmentation step only marginally increased the scan time of MS3 assays by 30 ms and did not compromise peptide throughput. Additionally, we quantified each phosphopeptide by high-resolution (7500 fwhm at 400 m/z (fwhm)) HCD fragmentation-based pSRM assays. Unfortunately, the instrument software did not support multistage activation-based pSRM-CID analysis[27,42] and therefore we could not include this popular phosphopeptide analysis technique in our comparison. Because only minor performance differences were observed in the first experiments between the DDA and INL approaches, we carried out only DDA analysis for the phosphopeptide samples.

Compared to unmodified peptides, the phosphopeptides analyzed generally showed a much higher variation, and higher

dx.doi.org/10.1021/pr500860c | J. Proteome Res. 2014, 13, 5973−5988

Table 1. Phosphopeptides Identified for the Protein Mad1

Best Ion Score [1]	Sequence	Precursor Ion Charge	Phosphosite Position	Phosphosite Reported Previously [2]	Putative Upstream Kinase(s)[3]
27.71	*S*LNNFISQR	2+	S16	Yes	Mps1, Plk1
34.77	IQELQA*S*QEAR	2+	S214	Yes	Mps1, Plk1, ATM kinase
33.02	DLEQKL*S*LQEQDAAIVK	3+	S233	No	
41.78	L*S*LQEQDAAIVK	2+	S233	No	
46.69	AILGSYDSELTPAEY*S*PQLTR	3+	S428	Yes	Mps1, Cdk1
54.81	AILGSYDSELTPAEY*S*PQLTR	2+	S428	Yes	Mps1, Cdk1
83.7	SQ*S*SSAEQSFLFSR	2+	S484	No	
56.79	SQS*S*SAEQSFLFSR	2+	S485	No	
68.94	SQSS*S*AEQSFLFSR	2+	S486	No	
72.63	SQSSSAEQ*S*FLFSR	2+	S490	Yes	Mps1, Plk1
31.74	SQSSSAEQSFLF*S*REEADTLR	3+	S494	No	
28.07	EEAD*T*LR	2+	T500	No	
21.74	LKVEELEGER*S*R	3+	S513	Yes	Mps1, (Plk1)
25.55	LKVEELEGER*S*R	2+	S513	Yes	Mps1, (Plk1)
24.27	VEELEGER*S*R	2+	S513	Yes	Mps1, (Plk1)
22.61	ALQGDYDQ*S*R	2+	S538	No	Mps1, (Plk1)
25.25	LREDH*S*QLQAECER	3+	S562	Yes	Mps1, (Plk1)

[1]Best ion score determined by the Mascot search engine. A detailed list of all identified MS/MS spectra is shown in Tables S20 and S21. [2]Obtained from www.phosphosite.org (20/05/2014). [3]Predicted consensus motifs for Mps1,[55,56] Plk1,[57,58] Cdk1,[58,59] and ATM/ATR[49,60] kinases.

LOD/LOQs were determined for all methods and samples (Figure 4E). In line with the results obtained for unmodified peptides, detection limits increased in the complex samples for all methods, most dramatically by 30-fold for the DDA approach and by 10-fold for SRM and pSRM-MS2-CID, and only little impact on LOD/LOQ values was observed for HCD (4-fold increase) and MS3 (2.5-fold increase) based pSRM strategies (Figure 4F). This can be mainly ascribed to the much smaller mass windows that could be applied for fragment ion extraction with HCD/Orbitrap MS2 scans and the additional isolation/fragmentation step for MS3 that considerably reduced noise and interfering peaks in the MS spectra. Figure S1 shows a typical phosphopeptide that was analyzed by all five methods with and without the presence of a human cell digest. We observed good linearity for all methods, with the MS3 method covering the largest dynamic concentration range for analyzing this phosphopeptide within a complex sample. The improved selectivity of HCD and MS3 can be illustrated with the transitions extracted for this peptide at 1 fmol concentration within a complex analytical background. Although DDA, SRM, and pSRM-CID-MS2 all showed very high noise levels and an accumulation of interfering peaks, the small mass extraction windows applied for pSRM-HCD-MS2 and the additional fragmentation step for the pSRM-CID-MS3 method considerably increased the selectivity and facilitated accurate peak interpretation (Figure S1L,O). Because the pSRM-CID-MS3 approach was not applicable to all phosphopeptides, due to missing neutral loss peaks, we set up a combined approach of MS2 and MS3 pSRM-CID-MS2 and selected the most sensitive assay for each peptide based on the complex sample series. This hybrid pSRM-MS2/MS3 method showed the lowest decrease in sensitivity upon increased sample complexity of only 2-fold (Figure 4F) and therefore also the lowest LODs/LOQs in the complex sample (Figure 4E).

To conclude, like that for unmodified peptides, the sensitivity of phosphopeptide detection critically depends on sample complexity for most approaches. High-resolution HCD fragmentation and, in particular, higher stage fragmentation (MS3) were found to be the most sensitive MS methods that were least affected by the analytical background. To demonstrate the power of this MS3 approach, we applied it to directly monitor phosphorylation changes in the mitotic spindle assembly checkpoint (SAC) protein Mad1 during cell cycle progression (see below).

Impact of Peptide Size on Limit of Detection/Quantification

Defining LODs/LOQs for 30 peptides allowed us to additionally evaluate the impact of general peptide properties on the sensitivity of the various MS methods tested. Interestingly, we found a strong and significant correlation between peptide length and LOD for all targeted, but not for MS1-based, DDA/INL LC−MS/MS methods. This was observed for the unmodified (Figure 5A−C) and phosphorylated (Figure 5D−F) peptides analyzed. Apparently, the higher number of fragment ions produced by longer peptides diluted the MS signal to many more ions compared to smaller peptides that generated fewer product ions. Intriguingly, no significant peptide length dependencies were found for precursor ion-based quantification methods (Figure 5A,D). This observation is further supported by a recent publication demonstrating a 3-fold loss of sensitivity when analyzing the same peptide using pSRM (fragment-based quantification) over single ion monitoring (precursor ion-based quantitation).[1] In this study, the impact of peptide size on assay sensitivity was even stronger for the peptides analyzed. On average, reducing peptide size by 8 amino acids lowered LOD for SRM and pSRM analysis by 1 order of magnitude for the unmodified and phosphorylated peptides (Figure 5). Therefore, focusing on smaller peptides could be an additional and easy to implement parameter to improve the sensitivity of MS assays for protein quantification. It is important to note that peptides selected for targeted analysis should not be too small so that a sufficient number of specific transitions is available for confident peak assignment, particularly if larger mass selection windows are applied.[46] Of note, with their high selectivity and specificity, the new HR/AM PRM approaches have demonstrated that confident peptide assignment can be achieved with as few as 3 transitions.[6] This makes this promising MS technology particularly well suited for the targeted analysis of shorter peptides.

dx.doi.org/10.1021/pr500860c | J. Proteome Res. 2014, 13, 5973−5988

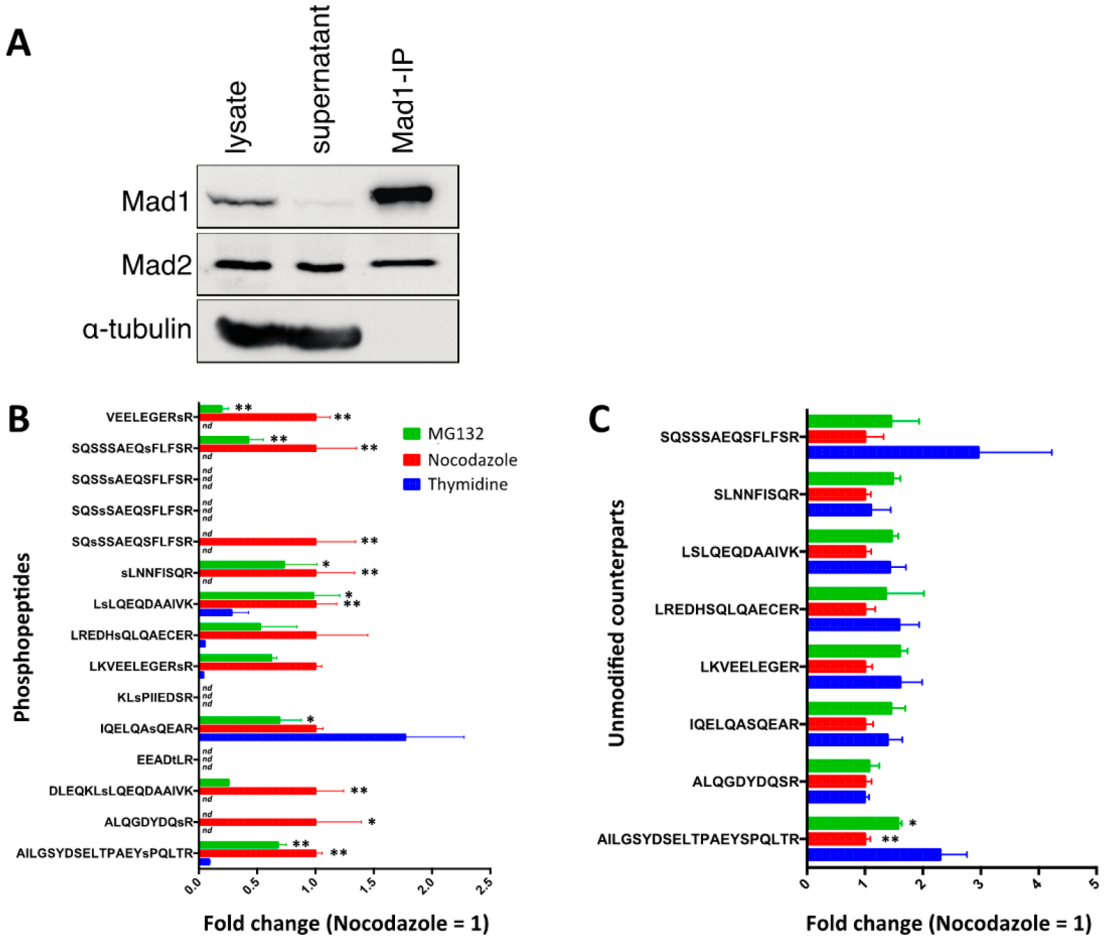

Figure 6. Quantification of all identified Mad1 phosphorylation sites across three different cell cycle stages. (A) Western blot of HeLa S3 cells synchronized with thymidine and subsequently released into nocodazole for 14 h. Cells were collected by mitotic shake-off, and Mad1 and associated proteins were immunopurified from mitotic extracts. (B) Bar chart showing the mean fold changes with error bars determined for each phosphopeptide quantified by pSRM-CID-MS2/MS3 of Mad1 immunopurified from thymidine (blue), nocodazole (red), and MG132 (green) arrested HeLa S3 cells. (C) Bar chart showing the mean abundance changes for the unmodified counterparts of the phosphopeptides monitored across the three different conditions. For clarity, the ratios for nocodazole were set to 1, and the other ratios were normalized accordingly. All experiments were carried out in triplicate. Significant changes are indicated (*, p-value < 0.05; **, p-value < 0.01; nd, no peaks detected).

Application to Mad1 Phosphorylation Site Monitoring

To demonstrate the power of the pSRM-CID-MS3 approach for sensitive phosphopeptide analysis, we applied it to monitor phosphorylation changes of the SAC protein Mad1 during cell cycle progression directly from pull-down experiments. Mad1 is one of the core proteins of the SAC, a surveillance mechanism that delays chromosome segregation until chromosome biorientation is achieved. Mad1, in complex with Mad2, transduces this wait anaphase signal at unattached kinetochores.[47] During interphase, Mad1 is located at the nucleoplasmic side of the nuclear envelope and then translocates to kinetochores after nuclear envelope breakdown (NEBD).[47,48]

Careful mapping of Mad1 phosphorylation sites at different cell cycle stages proved to be challenging. Although immunoprecipitation of Mad1 from mitotic cells was efficient (Figure 6A), phosphorylation events on Mad1 proved to be transient and/or of low stoichiometry. Thus, preliminary experiments showed that Mad1 phosphorylation analysis was not reproducible enough to consistently quantify all identified phosphopeptides across all samples (unpublished data). In addition, the high number of cells required for efficient phosphopeptide enrichment further complicated these experiments and increased the cost associated with sample preparation. Therefore, we applied the sensitive pSRM-CID-MS3 method to monitor all detectable Mad1 phosphorylation sites directly from minimal amounts of immunopurified Mad1 without phosphopeptide enrichment.

In a first step, we carried out an in-depth DDA MS analysis of phosphopeptides extracted from a pool of Mad1 immunopurifications obtained from each cell cycle state to generate an extensive catalogue of Mad1 phosphorylation sites. We identified a total of 17 unique phosphopeptide ions corresponding to 13 different phosphorylation sites, of which seven were previously unknown (Table 1). Subsequently, heavy-labeled reference peptides were synthesized for all identified phosphopeptides, and pSRM-CID-MS2/MS3 assays were generated for all phosphorylation sites as described above. No assay could be set up for S494 due to synthesis problems of the corresponding heavy reference peptide, and only the doubly charged precursor ion of the phosphopeptide AILGSYDSELTPAEYpSPQLTR covering S428 was included in the analysis. Overall, sensitive MS3-based pSRM assays could be generated for 13 of the 15 remaining phosphopeptide ions. Because several possible modification sites were in direct proximity of the peptide SQSSSAEQSFLFSR and high mascot scores were

dx.doi.org/10.1021/pr500860c | J. Proteome Res. 2014, 13, 5973−5988

obtained for four different sites, correct positioning of these phosphorylation sites was challenging (S484−S486 and S490, Table 1). Therefore, we first investigated whether we could obtain specific assays for each of the four phosphorylation sites. We selected specific and common fragments (Figure S2A) and analyzed them using pSRM-CID-MS3. As is apparent from Figure S2B−E, the four phosphopeptides showed different elution times and could be nearly fully resolved by the reversed-phase chromatography employed. Elution was the earlier the closer the phosphorylation was positioned to the peptide C-terminus, probably reflecting reduced interaction of the hydrophobic amino acids located at this part of the peptide with the stationary phase during LC. This allowed us to select, besides the few specific fragments, additional unspecific fragments with high MS intensities and generate sensitive, specific pSRM-CID-MS3 assays for all four phosphorylation sites (Figure S2B−E). In general, the pSRM method is particularly well-suited for localizing modifications of a particular peptide because, due to the same precursor ion mass, all possible sites can be monitored with one single MS assay.

Next, we employed these assays for extensive Mad1 phosphorylation site monitoring during three different cell cycle stages: S phase (achieved by thymidine addition), prometaphase (nocodazole treatment), where the SAC is active, and metaphase (MG132 addition), where the SAC is shut down. We could consistently detect and quantify 11 of the 15 targeted phosphopeptides (corresponding to 9 of the 13 identified phosphorylation sites) on endogenous Mad1 pulled-downs from cells in the three stages and across all biological replicates. We observed significant increases in phosphorylation for most sites after nocodazole and MG132 treatment compared to that after thymidine treatment (Figure 6B), in agreement with Mad1 function during SAC activation. According to the consensus motifs present on these phosphopeptides, Plk1, Mps1, and Cdk1 are likely candidate upstream kinases responsible for phosphorylating most of these sites in mitosis (Table 1). Interestingly, the peptide IQELQApSQEAR carrying a phosphorylation at serine 214 showed an opposite trend, namely, a clear increase during S phase (Figure 6B). Recently, this site has been shown to be phosphorylated by ATM kinase, and it has been suggested that such phosphorylation contributes to activation of the SAC.[49] In the future, it will be interesting to explore a possible role of serine 214 in the mitotic checkpoint complex assembly during interphase.

In an additional experiment, we analyzed each sample by shotgun DDA LC−MS/MS to quantify the unmodified counterparts of the phosphopeptides and define phosphorylation site stoichiometries. Here, we identified two phosphopeptides that showed a strong increase in phosphorylation occupancy of around 50% from S-phase to prometaphase and thus represent the most affected phosphorylation sites for the cell cycle stages analyzed (Figure 6C). It is important to note that with conventional DDA LC−MS/MS analysis only two phosphorylation sites of Mad1 could be identified and quantified from these pull-down samples by label-free quantification, whereas nine sites could be monitored by the more sensitive pSRM-CID-MS2/MS3 approach, increasing the coverage by 4.5-fold.

Knowing that Mad1 exerts its function mostly in the first half of mitosis and that Mad1 relocalizes from the nuclear envelope to unattached kinetochores,[50−52] it is tempting to speculate that such relocalization might depend on the phosphorylation status of Mad1.[53]

CONCLUSIONS

This is the first study that systematically assesses the performance of the most popular DDA and DIA MS approaches currently used in proteomics. The results will help users to select the most suitable LC−MS methods for their studies, to improve their experimental design, and to define reasonable expectations for future proteomics analyses. It is important to note that different MS analyzers and detectors, which were most suited for the individual MS workflows, were used throughout this study. Because not all LC−MS platforms were available for this study (e.g., fast scanning Orbitrap or time-of-flight analyzers for parallel reaction monitoring (PRM)[1,6]), users with a different LC−MS setup should carry out a similar method evaluation to assess the performance of their individual LC−MS platforms and workflows. Of note, a thorough comparison of the SRM (on QqQ instruments, used in this study) and PRM (on Orbitrap instruments) approaches has been described recently.[1,6]

In our study, we observed large performance differences in particular for phosphopeptide analyses in complex samples, and high-resolution HCD and higher stage fragmentation-based pSRM approaches were identified as the most sensitive approaches. We are confident that with the increasing number of known phosphorylation sites (or other PTMs) and the relatively low cost of synthetic heavy reference peptides with modification homologues, such extensive phosphorylation site or PTM monitoring studies can be applied to any protein of interest that can be enriched from a complex protein sample without the need for modification-specific enrichment steps.

ASSOCIATED CONTENT

Supporting Information

Figure S1: Defining linearity and detection and quantification limits for the phosphopeptide RDSLGpTYSSR. Figure S2: Generation of specific MS assays for the different phosphorylation sites identified for the peptide SQSSSAEQSFLFSR. Figure S3: Linearity, LODs, and LOQs for 20 unmodified peptides under neat and matrix-containing conditions targeted in pSRM-CID-MS2 experiments. Figure S4: Linearity, LODs, and LOQs for 20 unmodified peptides under neat and matrix-containing conditions targeted in SRM experiments. Figure S5: Linearity, LODs, and LOQs for 20 unmodified peptides under neat and matrix-containing conditions targeted in INL experiments. Figure S6: Linearity, LODs, and LOQs for 20 unmodified peptides under neat and matrix-containing conditions targeted in DDA experiments. Figure S7: Linearity, LODs, and LOQs for 10 phosphopeptides under neat and matrix-containing conditions targeted in pSRM-CID-MS2 experiments. Figure S8: Linearity, LODs, and LOQs for 10 phosphopeptides under neat and matrix-containing conditions targeted in pSRM-HCD-MS2 experiments. Figure S9: Linearity, LODs, and LOQs for 10 phosphopeptides under neat and matrix-containing conditions targeted in SRM experiments. Figure S10: Linearity, LODs, and LOQs for 10 phosphopeptides under neat and matrix-containing conditions targeted in pSRM-CID-MS3 experiments. Figure S11: Linearity, LODs, and LOQs for 10 phosphopeptides under neat and matrix-containing conditions targeted in DDA experiments. Table S1: Peptide sequences employed for dilution curve experiments.

dx.doi.org/10.1021/pr500860c | J. Proteome Res. 2014, 13, 5973−5988

Table S2: Inclusion mass list used for INL-based analysis of unmodified reference peptides. Table S3: Inclusion mass list used for INL-based analysis of reference phosphopeptides. Table S4: Transition list with optimized collision energies for SRM analysis of unmodified reference peptides. Table S5: Transition list with optimized collision energies for SRM analysis of reference phosphopeptides. Table S6: Integrated peak areas determined by the Skyline software for unmodified reference peptide samples analyzed by DDA. Table S7: Integrated peak areas determined by the Skyline software for unmodified reference peptide samples analyzed by INL. Table S8: Integrated peak areas determined by the Skyline software for unmodified reference peptide samples analyzed by SRM using a QqQ instrument. Table S9: Integrated peak areas determined by the Skyline software for unmodified reference peptide samples analyzed by pSRM using a LIT instrument. Table S10: Integrated peak areas determined by the Skyline software for reference phosphopeptide samples analyzed by DDA. Table S11: Integrated peak areas determined by the Skyline software for reference phosphopeptide samples analyzed by SRM using a QqQ instrument. Table S12: Integrated peak areas determined by the Skyline software for reference phosphopeptide samples analyzed by pSRM-HCD. Table S13: Integrated peak areas determined by the Skyline software for reference phosphopeptide samples analyzed by pSRM-CID-MS2. Table S14: Integrated peak areas determined by the Skyline software for reference phosphopeptide samples analyzed by pSRM-CID-MS3. Tables S15−S17: Unmodified reference peptides identified in dilution series samples by database searching using DDA, INL, and pSRM analysis. Tables S18−S20: Identified proteins, peptides, and MS/MS spectra of a Mad1 phosphorylation site catalogue from phosphopeptide enriched samples. Table S21: List of all MS/MS spectra assigned to Mad1 phosphopeptides. Tables S22 and S23: Quantitative results of Mad1 phosphorylation site monitoring, including normalization, ratio determination, and statistical analysis. Table S24: List of All identified and quantified peptides for Mad1 phosphorylation site monitoring. Table S25: Data file names of LC−MS runs of all samples analyzed in this study. This material is available free of charge via the Internet at http://pubs.acs.org.

AUTHOR INFORMATION

Corresponding Author

*E-mail: alex.schmidt@unibas.ch. Phone: +41 61 267 20 59. Fax: +41 61 267 20 09.

Present Addresses

[‡]Division of Developmental Immunology Biocenter, Innsbruck Medical University, Innrain 80, 6020 Innsbruck, Austria.

[§]Cell Cycle and Mitosis Laboratory, Research Unit in Biomedicine and Translational Oncology, Vall Hebron Institute of Research, Psg. Vall d'Hebron 119-129, 08035 Barcelona, Spain.

Author Contributions

[†]M.B., E.A., and A.P.B. contributed equally to this work.

Notes

The authors declare no competing financial interest.

ACKNOWLEDGMENTS

We thank Roman Koerner (MPI for Biochemistry, Martinsried, Germany) for data sharing during the initial LC−MS experiments on Mad1 and all members of the Biozentrum's Proteomics Core Facility and the Nigg laboratory for helpful discussions. M.B. and E.A.N. were supported by the Swiss National Science Foundation (31003A_132428 and 310030B_149641), and A.P.B., by the Fellowships for Excellence Ph.D. Program of the Werner Siemens Foundation and the University of Basel.

ABBREVIATIONS

DDA, data-dependent acquisition; DIA, data-independent acquisition; PRM, parallel reaction monitoring; MRM, multiple reaction monitoring; SRM, selected reaction monitoring; pSRM, pseudo-selected reaction monitoring; QqQ, triple quadrupole; HR/AM, high resolution/accurate mass; CID, collision induced dissociation; HCD, higher energy c-trap dissociation; SAC, spindle assembly checkpoint; LOD, limit of detection; LOQ, limit of quantification; LOI, limit of identification; PTM, post-translational modification; fwhm, full width at half-maximum; LIT, linear ion trap; LFQ, label-free quantification; BG, background

REFERENCES

(1) Gallien, S.; Duriez, E.; Crone, C.; Kellmann, M.; Moehring, T.; Domon, B. Targeted proteomic quantification on quadrupole-orbitrap mass spectrometer. *Mol. Cell. Proteomics* **2012**, *11*, 1709−1723.

(2) Simicevic, J.; Schmid, A. W.; Gilardoni, P. A.; Zoller, B.; Raghav, S. K.; Krier, I.; Gubelmann, C.; Lisacek, F.; Naef, F.; Moniatte, M. Absolute quantification of transcription factors during cellular differentiation using multiplexed targeted proteomics. *Nat. Methods* **2013**, *10*, 570−576.

(3) Nagaraj, N.; Wiśniewski, J. R.; Geiger, T.; Cox, J.; Kircher, M.; Kelso, J.; Pääbo, S.; Mann, M. Deep proteome and transcriptome mapping of a human cancer cell line. *Mol. Syst. Biol.* **2011**, *7*, 548.

(4) Beck, M.; Claassen, M.; Aebersold, R. Comprehensive proteomics. *Curr. Opin. Biotechnol.* **2011**, *22*, 3−8.

(5) Domon, B.; Aebersold, R. Options and considerations when selecting a quantitative proteomics strategy. *Nat. Biotechnol.* **2010**, *28*, 710−721.

(6) Peterson, A. C.; Russell, J. D.; Bailey, D. J.; Westphall, M. S.; Coon, J. J. Parallel reaction monitoring for high resolution and high mass accuracy quantitative, targeted proteomics. *Mol. Cell. Proteomics* **2012**, *11*, 1475−1488.

(7) Sandhu, C.; Hewel, J. A.; Badis, G.; Talukder, S.; Liu, J.; Hughes, T. R.; Emili, A. Evaluation of data-dependent versus targeted shotgun proteomic approaches for monitoring transcription factor expression in breast cancer. *J. Proteome Res.* **2008**, *7*, 1529−1541.

(8) Michalski, A.; Cox, J.; Mann, M. More than 100,000 detectable peptide species elute in single shotgun proteomics runs but the majority is inaccessible to data-dependent LC−MS/MS. *J. Proteome Res.* **2011**, *10*, 1785−1793.

(9) Picotti, P.; Aebersold, R. Selected reaction monitoring-based proteomics: workflows, potential, pitfalls and future directions. *Nat. Methods* **2012**, *9*, 555−566.

(10) Schmidt, A.; Gehlenborg, N.; Bodenmiller, B.; Mueller, L. N.; Campbell, D.; Mueller, M.; Aebersold, R.; Domon, B. An integrated, directed mass spectrometric approach for in-depth characterization of complex peptide mixtures. *Mol. Cell. Proteomics* **2008**, *7*, 2138−2150.

(11) Jaffe, J. D.; Keshishian, H.; Chang, B.; Addona, T. A.; Gillette, M. A.; Carr, S. A. Accurate inclusion mass screening: a bridge from unbiased discovery to targeted assay development for biomarker verification. *Mol. Cell. Proteomics* **2008**, *7*, 1952−1962.

(12) Fava, L. L.; Kaulich, M.; Nigg, E. A.; Santamaria, A. Probing the in vivo function of Mad1:C-Mad2 in the spindle assembly checkpoint. *EMBO J.* **2011**, *30*, 3322−3336.

(13) Gillette, M. A.; Carr, S. A. Quantitative analysis of peptides and proteins in biomedicine by targeted mass spectrometry. *Nat. Methods* **2013**, *10*, 28−34.

(14) Savitski, M. M.; Fischer, F.; Mathieson, T.; Sweetman, G.; Lang, M.; Bantscheff, M. Targeted data acquisition for improved reproducibility and robustness of proteomic mass spectrometry assays. *J. Am. Soc. Mass Spectrom.* **2010**, *21*, 1668−1679.
(15) Schmidt, A.; Beck, M.; Malmstrom, J.; Lam, H.; Claassen, M.; Campbell, D.; Aebersold, R. Absolute quantification of microbial proteomes at different states by directed mass spectrometry. *Mol. Syst. Biol.* **2011**, *7*, 510.
(16) Picotti, P.; Bodenmiller, B.; Mueller, L. N.; Domon, B.; Aebersold, R. Full dynamic range proteome analysis of *S. cerevisiae* by targeted proteomics. *Cell* **2009**, *138*, 795−806.
(17) Maclean, B.; Tomazela, D. M.; Shulman, N.; Chambers, M.; Finney, G. L.; Frewen, B.; Kern, R.; Tabb, D. L.; Liebler, D. C.; Maccoss, M. J. Skyline: an open source document editor for creating and analyzing targeted proteomics experiments. *Bioinformatics* **2010**, *26*, 966−968.
(18) Hebert, A. S.; Richards, A. L.; Bailey, D. J.; Ulbrich, A.; Coughlin, E. E.; Westphall, M. S.; Coon, J. J. The one hour yeast proteome. *Mol. Cell. Proteomics* **2013**, *13*, 339−347.
(19) Anderson, D. J. Determination of the lower limit of detection. *Clin. Chem.* **1989**, *35*, 2152−2153.
(20) Shi, T.; Fillmore, T. L.; Sun, X.; Zhao, R.; Schepmoes, A. A.; Hossain, M.; Xie, F.; Wu, S.; Kim, J.-S.; Jones, N.; et al. Antibody-free, targeted mass-spectrometric approach for quantification of proteins at low picogram per milliliter levels in human plasma/serum. *Proc. Natl. Acad. Sci. U.S.A.* **2012**, *109*, 15395−15400.
(21) Schmidt, A.; Claassen, M.; Aebersold, R. Directed mass spectrometry: towards hypothesis-driven proteomics. *Curr. Opin. Chem. Biol.* **2009**, *13*, 510−517.
(22) Anderson, N. L.; Anderson, N. G.; Haines, L. R.; Hardie, D. B.; Olafson, R. W.; Pearson, T. W. Mass spectrometric quantitation of peptides and proteins using stable isotope standards and capture by anti-peptide antibodies (SISCAPA). *J. Proteome Res.* **2004**, *3*, 235−244.
(23) Makarov, A.; Denisov, E.; Lange, O.; Horning, S. Dynamic range of mass accuracy in LTQ Orbitrap hybrid mass spectrometer. *J. Am. Soc. Mass Spectrom.* **2006**, *17*, 977−982.
(24) Burgess, M. W.; Keshishian, H.; Mani, D. R.; Gillette, M. A.; Carr, S. A. Simplified and efficient quantification of low abundance proteins at very high multiplex by targeted mass spectrometry. *Mol. Cell. Proteomics* **2014**, *13*, 1137−1149.
(25) Lange, V.; Picotti, P.; Domon, B.; Aebersold, R. Selected reaction monitoring for quantitative proteomics: a tutorial. *Mol. Syst. Biol.* **2008**, *4*, 222.
(26) Kulasingam, V.; Smith, C. R.; Batruch, I.; Buckler, A.; Jeffery, D. A.; Diamandis, E. P. "Product ion monitoring" assay for prostate-specific antigen in serum using a linear ion-trap. *J. Proteome Res.* **2008**, *7*, 640−647.
(27) Addona, T. A.; Abbatiello, S. E.; Schilling, B.; Skates, S. J.; Mani, D. R.; Bunk, D. M.; Spiegelman, C. H.; Zimmerman, L. J.; Ham, A.-J. L.; Keshishian, H.; et al. Multi-site assessment of the precision and reproducibility of multiple reaction monitoring-based measurements of proteins in plasma. *Nat. Biotechnol.* **2009**, *27*, 633−641.
(28) Picotti, P.; Lam, H.; Campbell, D.; Deutsch, E. W.; Mirzaei, H.; Ranish, J.; Domon, B.; Aebersold, R. A database of mass spectrometric assays for the yeast proteome. *Nat. Methods* **2008**, *5*, 913−914.
(29) Picotti, P.; Clément-Ziza, M.; Lam, H.; Campbell, D. S.; Schmidt, A.; Deutsch, E. W.; Röst, H.; Sun, Z.; Rinner, O.; Reiter, L.; et al. A complete mass-spectrometric map of the yeast proteome applied to quantitative trait analysis. *Nature* **2013**, *494*, 266−270.
(30) Schubert, O. T.; Mouritsen, J.; Ludwig, C.; Röst, H. L.; Rosenberger, G.; Arthur, P. K.; Claassen, M.; Campbell, D. S.; Sun, Z.; Farrah, T.; et al. The Mtb proteome library: a resource of assays to quantify the complete proteome of *Mycobacterium tuberculosis*. *Cell Host Microbe* **2013**, *13*, 602−612.
(31) Cox, J.; Neuhauser, N.; Michalski, A.; Scheltema, R. A.; Olsen, J. V.; Mann, M. Andromeda: a peptide search engine integrated into the MaxQuant environment. *J. Proteome Res.* **2011**, *10*, 1794−1805.
(32) Chen, X.; Drogaris, P.; Bern, M. Identification of tandem mass spectra of mixtures of isomeric peptides. *J. Proteome Res.* **2010**, *9*, 3270−3279.
(33) Jorge, I.; Casas, E. M.; Villar, M.; Ortega-Pérez, I.; López-Ferrer, D.; Martínez-Ruiz, A.; Carrera, M.; Marina, A.; Martínez, P.; Serrano, H.; et al. High-sensitivity analysis of specific peptides in complex samples by selected MS/MS ion monitoring and linear ion trap mass spectrometry: application to biological studies. *J. Mass Spectrom.* **2007**, *42*, 1391−1403.
(34) Nesvizhskii, A. I.; Keller, A.; Kolker, E.; Aebersold, R. A statistical model for identifying proteins by tandem mass spectrometry. *Anal. Chem.* **2003**, *75*, 4646−4658.
(35) Vizcaíno, J. A.; Côté, R. G.; Csordas, A.; Dianes, J. A.; Fabregat, A.; Foster, J. M.; Griss, J.; Alpi, E.; Birim, M.; Contell, J.; et al. The PRoteomics IDEntifications (PRIDE) database and associated tools: status in 2013. *Nucleic Acids Res.* **2013**, *41*, D1063−D1069.
(36) Glatter, T.; Ludwig, C.; Ahrné, E.; Aebersold, R.; Heck, A. J. R.; Schmidt, A. Large-scale quantitative assessment of different in-solution protein digestion protocols reveals superior cleavage efficiency of tandem Lys-C/trypsin proteolysis over trypsin digestion. *J. Proteome Res.* **2012**, *11*, 5145−5156.
(37) Pak, H.; Nikitin, F.; Gluck, F.; Lisacek, F.; Scherl, A.; Müller, M. Clustering and filtering tandem mass spectra acquired in data-independent mode. *J. Am. Soc. Mass Spectrom.* **2013**, *24*, 1862−1871.
(38) Reiter, L.; Rinner, O.; Picotti, P.; Hüttenhain, R.; Beck, M.; Brusniak, M.-Y.; Hengartner, M. O.; Aebersold, R. mProphet: automated data processing and statistical validation for large-scale SRM experiments. *Nat. Methods* **2011**, *8*, 430−435.
(39) Gillet, L. C.; Navarro, P.; Tate, S.; Röst, H.; Selevsek, N.; Reiter, L.; Bonner, R.; Aebersold, R. Targeted data extraction of the MS/MS spectra generated by data-independent acquisition: a new concept for consistent and accurate proteome analysis. *Mol. Cell. Proteomics* **2012**, *11*, O111.016717.
(40) Hanke, S.; Besir, H.; Oesterhelt, D.; Mann, M. Absolute SILAC for accurate quantitation of proteins in complex mixtures down to the attomole level. *J. Proteome Res.* **2008**, *7*, 1118−1130.
(41) Olsen, J. V.; Blagoev, B.; Gnad, F.; Macek, B.; Kumar, C.; Mortensen, P.; Mann, M. Global, in vivo, and site-specific phosphorylation dynamics in signaling networks. *Cell* **2006**, *127*, 635−648.
(42) Ulintz, P. J.; Yocum, A. K.; Bodenmiller, B.; Aebersold, R.; Andrews, P. C.; Nesvizhskii, A. I. Comparison of MS^2-only, MSA, and MS^2/MS^3 methodologies for phosphopeptide identification. *J. Proteome Res.* **2009**, *8*, 887−899.
(43) Olsen, J. V.; Macek, B.; Lange, O.; Makarov, A.; Horning, S.; Mann, M. Higher-energy C-trap dissociation for peptide modification analysis. *Nat. Methods* **2007**, *4*, 709−712.
(44) Palumbo, A. M.; Tepe, J. J.; Reid, G. E. Mechanistic insights into the multistage gas-phase fragmentation behavior of phosphoserine- and phosphothreonine-containing peptides. *J. Proteome Res.* **2008**, *7*, 771−779.
(45) Sherrod, S. D.; Myers, M. V.; Li, M.; Myers, J. S.; Carpenter, K. L.; Maclean, B.; Maccoss, M. J.; Liebler, D. C.; Ham, A.-J. L. Label-free quantitation of protein modifications by pseudo selected reaction monitoring with internal reference peptides. *J. Proteome Res.* **2012**, *11*, 3467−3479.
(46) Rost, H. L.; Malmström, L.; Aebersold, R. A computational tool to detect and avoid redundancy in selected reaction monitoring. *Mol. Cell. Proteomics* **2012**, *11*, 540−549.
(47) Foley, E. A.; Kapoor, T. M. Microtubule attachment and spindle assembly checkpoint signalling at the kinetochore. *Nat. Rev. Mol. Cell Biol.* **2013**, *14*, 25−37.
(48) Musacchio, A.; Salmon, E. D. The spindle-assembly checkpoint in space and time. *Nat. Rev. Mol. Cell Biol.* **2007**, *8*, 379−393.
(49) Yang, C.; Hao, J.; Kong, D.; Cui, X.; Zhang, W.; Wang, H.; Guo, X.; Ma, S.; Liu, X.; Pu, P. ATM-mediated Mad1 serine 214 phosphorylation regulates Mad1 dimerization and the spindle assembly checkpoint. *Carcinogenesis* **2014**, *35*, 2007−2013.

(50) Campbell, M. S.; Chan, G. K.; Yen, T. J. Mitotic checkpoint proteins HsMAD1 and HsMAD2 are associated with nuclear pore complexes in interphase. *J. Cell Sci.* **2001**, *114*, 953−963.
(51) Iouk, T.; Kerscher, O.; Scott, R. J.; Basrai, M. A.; Wozniak, R. W. The yeast nuclear pore complex functionally interacts with components of the spindle assembly checkpoint. *J. Cell Biol.* **2002**, *159*, 807−819.
(52) Rodriguez-Bravo, V.; Maciejowski, J.; Corona, J.; Buch, H. K.; Collin, P.; Kanemaki, M. T.; Shah, J. V.; Jallepalli, P. V. Nuclear pores protect genome integrity by assembling a premitotic and mad1-dependent anaphase inhibitor. *Cell* **2014**, *156*, 1017−1031.
(53) Funabiki, H.; Wynne, D. J. Making an effective switch at the kinetochore by phosphorylation and dephosphorylation. *Chromosoma* **2013**, *122*, 135−158.
(54) Pappin, D. J.; Hojrup, P.; Bleasby, A. J. Rapid identification of proteins by peptide-mass fingerprinting. *Curr. Biol.* **1993**, *3*, 327−332.
(55) Dou, Z.; von Schubert, C.; Körner, R.; Santamaria, A.; Elowe, S.; Nigg, E. A. Quantitative mass spectrometry analysis reveals similar substrate consensus motif for human Mps1 kinase and Plk1. *PLoS One* **2011**, *6*, e18793.
(56) Hennrich, M. L.; Marino, F.; Groenewold, V.; Kops, G. J. P. L.; Mohammed, S.; Heck, A. J. R. Universal quantitative kinase assay based on diagonal SCX chromatography and stable isotope dimethyl labeling provides high-definition kinase consensus motifs for PKA and human Mps1. *J. Proteome Res.* **2013**, *12*, 2214−2224.
(57) Santamaria, A.; Wang, B.; Elowe, S.; Malik, R.; Zhang, F.; Bauer, M.; Schmidt, A.; Silljé, H. H. W.; Körner, R.; Nigg, E. A. The Plk1-dependent phosphoproteome of the early mitotic spindle. *Mol. Cell. Proteomics* **2011**, *10*, M110.004457.
(58) Alexander, J.; Lim, D.; Joughin, B. A.; Hegemann, B.; Hutchins, J. R. A.; Ehrenberger, T.; Ivins, F.; Sessa, F.; Hudecz, O.; Nigg, E. A.; et al. Spatial exclusivity combined with positive and negative selection of phosphorylation motifs is the basis for context-dependent mitotic signaling. *Sci. Signaling* **2011**, *4*, ra42.
(59) Elia, A. E. H.; Cantley, L. C.; Yaffe, M. B. Proteomic screen finds pSer/pThr-binding domain localizing Plk1 to mitotic substrates. *Science* **2003**, *299*, 1228−1231.
(60) Traven, A.; Heierhorst, J. SQ/TQ cluster domains: concentrated ATM/ATR kinase phosphorylation site regions in DNA-damage-response proteins. *BioEssays* **2005**, *27*, 397−407.